A. Papandreou-Suppappola, F. Hlawatsch, and G. F. Boudreaux-Bartels,
Power class time-frequency representations and their applications,
in Time-Frequency Signal Analysis and Processing: A Comprehensive Reference,
ed. B. Boashash, Oxford, UK: Elsevier, 2003, ch. 15.3, pp. 643–650.

15.3 POWER CLASS TIME-FREQUENCY REPRESENTATIONS AND THEIR APPLICATIONS[0]

15.3.1 Power Class Quadratic Time-Frequency Representations

Various classes of quadratic time-frequency representations (QTFRs) are best suited for analyzing signals with certain types of time-frequency (TF) geometries. For example, when a signal has constant TF characteristics, Cohen's class QTFRs (with signal-independent kernels) [3] [4] are most appropriate. The aforementioned QTFR classification is based on the grouping together of all QTFRs that satisfy the same two signal transformation covariance properties (see Articles 4.3 and 5.6 and [5] [11]). Specifically, Cohen's class [3] [4] consists of QTFRs that are covariant to constant (nondispersive) time shifts and frequency shifts of the signal whereas the affine class (see Article 7.1 and [4] [12] [2]) consists of QTFRs that are covariant to scale changes (dilations) and constant time shifts. Furthermore, the hyperbolic class [9] [6] consists of QTFRs that are covariant to scale changes and hyperbolic dispersive time shifts and are best suited to analyze signals with hyperbolic (nonlinear) group delay. When the analysis signal has a group delay that is a power function of frequency, the aforementioned QTFRs do not provide an adequate representation as they do not match power TF characteristics. Thus, we designed *power class* QTFRs to successfully localize signals along their power law group delay functions [7] [10].

The importance of power QTFRs is pronounced by the fact that many applications involve signals with dispersive group delays governed by a power law that corresponds to some power parameter κ. Examples of such signals include the dispersive propagation of a shock wave in a steel beam ($\kappa = 1/2$), trans-ionospheric chirps measured by satellites ($\kappa = -1$), acoustical waves reflected from a spherical shell immersed in water, various cetacean mammal whistles, and signal solutions of the diffusion equation ($\kappa = 1/2$) (e.g., waves propagating along uniform distributed RC transmission lines). Power laws can also be used to roughly approximate other, more complex, group delays. References for these applications can be found in [7].

Localized signal analysis application. The type of signals found in the applications mentioned above constitute the family of *power impulses* that best typifies the power TF geometry. Power impulses are defined in the frequency domain as

$$I_c^{(\kappa)}(f) \triangleq \sqrt{|\tau_\kappa(f)|}\, e^{-j2\pi c\, \Lambda_\kappa\left(\frac{f}{f_r}\right)} = \sqrt{(|\kappa|/f_r)\,|f/f_r|^{\kappa-1}}\, e^{-j2\pi c\, \mathrm{sgn}(f)|f/f_r|^\kappa} \quad (15.3.1)$$

with monotonic phase spectrum $\Lambda_\kappa(f/f_r) = \mathrm{sgn}(f)\,|f/f_r|^\kappa$ and power group delay

[0]Authors: **Antonia Papandreou-Suppappola**, Telecommunications Research Center, Department of Electrical Engineering, Arizona State University, Tempe, AZ 85287-7206 USA (papandreou@asu.edu), **Franz Hlawatsch**, Institute of Communications and Radio-Frequency Engineering, Vienna University of Technology, A-1040 Vienna, Austria (fhlawats@pop.tuwien.ac.at), and **G. Faye Boudreaux-Bartels**, Department of Electrical and Computer Engineering, University of Rhode Island, Kingston, RI 02881 USA (boud@ele.uri.edu). This work was supported in part by FWF grants P12228-ÖPH and J0530-TEC, and by ONR grant N00014-96-1-0350.
Reviewers: J. Bertrand and J. P. Ovarlez.

$\tau_g(f) = c\,\tau_\kappa(f) = c\,\frac{|\kappa|}{f_r}\,|f/f_r|^{\kappa-1} = c\,\frac{d}{df}\Lambda_\kappa(f/f_r)$ with $f \in \Re$. Here, $\mathrm{sgn}(f)$ provides the sign (± 1) of the frequency variable f, and $f_r > 0$ is a fixed reference frequency. For successful analysis, an ideal QTFR T must be localized along the group delay $\tau_g(f)$ of the power impulse in Equation (15.3.1). In particular,

$$T_{I_c^{(\kappa)}}(t,f) = |\tau_\kappa(f)|\;\delta\big(t - c\,\tau_\kappa(f)\big) \tag{15.3.2}$$

is very desirable in many applications where information about the signal analyzed could be obtained from the localized curve $t = c\,\tau_\kappa(f)$ in the TF plane. For example, the localization could be used in applications such as signal classification or estimation of the parameter c in (15.3.1). As we will show next, some power class QTFRs ideally provide the localized representation in (15.3.2) for analyzing power impulses as well as other signals with power group delay.

The power law TF structure can also be observed in applications where a system can cause a time shift that varies dispersively in frequency to an input signal with Fourier transform $X(f)$ yielding the output signal $Y(f) = e^{-j2\pi c\Lambda_\kappa(f/f_r)}\,X(f)$. Thus, power QTFRs could be used successfully in applications where a signal with constant group delay passes through a system with power dispersive TF characteristics that transforms the signal's constant group delay to a power group delay [7]. For example, the ocean is a medium (system) that could cause power dispersive changes to an underwater communications information message and its echoes. These changes could be accounted for at the receiver when matching processing tools, like power QTFRs, are used for detection.

The power QTFR classes. Following the covariance-based classification method, for an analysis signal $x(t)$ with Fourier spectrum $X(f)$, we define all κth power class QTFRs, $T_X^{(\kappa)}(t,f)$, to satisfy two specific covariance properties [7] [10]. The first property is covariance to scale changes on $x(t)$, i.e.,

$$T_{\mathcal{C}_a X}^{(\kappa)}(t,f) \;=\; T_X^{(\kappa)}(at, f/a)\,, \tag{15.3.3}$$

where the scaling operator $\mathcal{C}_a$ is defined as $(\mathcal{C}_a X)(f) = X(f/a)\,/\sqrt{|a|}$. The second property is covariance to power time shifts on $x(t)$ that correspond to frequency-dependent shifts, $\tau_\kappa(f)$, in the signal's group delay . Specifically,

$$T_{\mathcal{D}_c^{(\kappa)} X}^{(\kappa)}(t,f) \;=\; T_X^{(\kappa)}\big(t - c\,\tau_\kappa(f), f\big) \;=\; T_X^{(\kappa)}\left(t - c\,(\kappa/f_r)|f/f_r|^{\kappa-1},\; f\right) \tag{15.3.4}$$

for $f \in \Re$. The effect of the power time shift operator $\mathcal{D}_c^{(\kappa)}$ is given by [7]

$$(\mathcal{D}_c^{(\kappa)} X)(f) = e^{-j2\pi c\,\Lambda_\kappa(f/f_r)}\,X(f) = e^{-j2\pi c\,\mathrm{sgn}(f)|f/f_r|^\kappa}\,X(f)\,. \tag{15.3.5}$$

Here, $c \in \Re$ and $\kappa \in \Re$ ($\kappa \neq 0$) is the power parameter associated with each power class. The κth power function $\Lambda_\kappa(b) = \mathrm{sgn}(b)\,|b|^\kappa$, $b \in \Re$, corresponds[1] to a

[1]The definition $\Lambda_\kappa(b) = \mathrm{sgn}(b)\,|b|^\kappa$ versus $\Lambda_\kappa(b) = b^\kappa$ extends the power function to $b < 0$ so that $\Lambda_\kappa(b)$ is an odd, strictly monotonic function constituting a one-to-one mapping from $\Re$ to $\Re$.

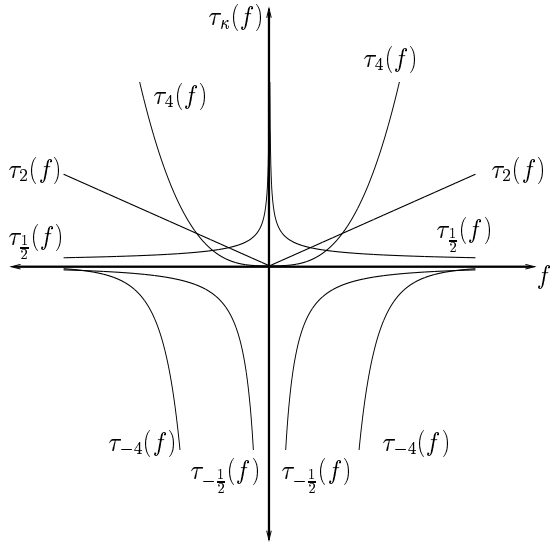

Figure 15.1: The power group delay $\tau_\kappa(f)$ for various choices of the power parameter κ.

transformation of the phase spectrum of the signal as shown in Equation (15.3.5). The frequency-dependent time shift $\tau_\kappa(f)$ in (15.3.4) corresponds to the derivative of the power function, i.e., $\tau_\kappa(f) = \frac{d}{df}\Lambda_\kappa(f/f_r) = \frac{\kappa}{f_r}|f/f_r|^{\kappa-1}$. Fig. 15.1 depicts $\tau_\kappa(f)$ in the TF plane for various choices of the power parameter κ.

The importance of the κth power class QTFRs is directly linked to the two covariances in (15.3.3) and (15.3.4). The power time shift covariance in (15.3.4) is useful in analyzing signals passing through dispersive systems with power law group delay or signals localized along power law curves in the TF plane. On the other hand, the scale covariance in (15.3.3) is important for multiresolution analysis.

Power class formulation. It was shown in [7] that any QTFR of the κth power class can be expressed as

$$T_X^{(\kappa)}(t,f) = \frac{1}{|f|}\int_{-\infty}^{\infty}\int_{-\infty}^{\infty}\Gamma_T(f_1/f, f_2/f) \cdot e^{j2\pi(tf/\kappa)[\Lambda_\kappa(f_1/f)-\Lambda_\kappa(f_2/f)]}\, X(f_1)\, X^*(f_2)\, df_1\, df_2\,, \qquad (15.3.6)$$

where the two-dimensional (2-D) kernel $\Gamma_T(b_1, b_2)$ uniquely characterizes the QTFR. Specific choices of $\Gamma_T(b_1, b_2)$ define specific QTFRs $T^{(\kappa)}$ in the κth power class. Also note that a different power class is obtained by varying κ in (15.3.6). When $\kappa = 1$, the affine class is obtained which is an important special case of the power classes corresponding to the constant (nondispersive) time shift $\tau_1(f) \equiv 1/f_r$.

The κth power class QTFR in (15.3.6) can also be obtained via a unitary warping operation (see Articles 4.5 and 5.6 and [7] [10] [1]). Specifically, if $T_X^{(A)}(t,f)$ is a QTFR of the affine class, then the corresponding κth power class QTFR, $T_X^{(\kappa)}(t,f)$,

can be obtained by warping the affine class QTFR, $T_X^{(A)}(t,f)$, according to [7]

$$\begin{aligned} T_X^{(\kappa)}(t,f) &= T_{\mathcal{U}_\kappa X}^{(A)}\left(\frac{t}{f_r \tau_\kappa(f)}, f_r \Lambda_\kappa(f/f_r)\right) \\ &= T_{\mathcal{U}_\kappa X}^{(A)}\left(\frac{t}{\kappa |f/f_r|^{\kappa-1}}, f_r \mathrm{sgn}(f) |f/f_r|^\kappa\right). \end{aligned} \tag{15.3.7}$$

Here, the unitary[2] frequency axis warping operator [7] [10] $\mathcal{U}_\kappa$ is given by

$$(\mathcal{U}_\kappa X)(f) = \frac{X\left(f_r \Lambda_\kappa^{-1}(f/f_r)\right)}{\sqrt{f_r \left|\tau_\kappa\left(f_r \Lambda_\kappa^{-1}(f/f_r)\right)\right|}} = \frac{1}{\sqrt{|\kappa|} |f/f_r|^{\frac{\kappa-1}{2\kappa}}} X\left(f_r \mathrm{sgn}(f) |f/f_r|^{\frac{1}{\kappa}}\right)$$

where the inverse function $\Lambda_\kappa^{-1}(b)$ satisfies $\Lambda_\kappa^{-1}(\Lambda_\kappa(b)) = \Lambda_\kappa(\Lambda_\kappa^{-1}(b)) = b$. The QTFRs of the affine class are defined as [4]

$$T_X^{(A)}(t,f) = \frac{1}{|f|} \int_{-\infty}^{\infty} \int_{-\infty}^{\infty} \Gamma_T(f_1/f, f_2/f)\, e^{j2\pi t(f_1-f_2)}\, X(f_1)\, X^*(f_2)\, df_1 df_2\,,$$

where $\Gamma_T(b_1,b_2)$ is a 2-D kernel characterizing the affine class QTFR (cf. (15.3.6)). Note that $T_X^{(A)}(t,f) = T_X^{(\kappa)}(t,f)\big|_{\kappa=1}$. The unitary warping relation in (15.3.7) preserves certain desirable characteristics of the affine class while transforming other ones to match the dispersive nature of the signals to be analyzed by power class QTFRs. For example, whereas both classes preserve scale changes of the signal, only the affine class preserves constant (nondispersive) time shifts. On the other hand, the warping in (15.3.7) transforms constant time shifts to power dispersive time shifts in the power class, and thus the constant time shift covariance of the affine class is transformed into the power time shift covariance of the power classes. The warping also provides an efficient method for computing power class QTFRs when algorithms for computing affine class QTFRs are available [10].

Class members. Specific QTFRs of the power classes satisfy various desirable properties in addition to the covariance properties in (15.3.3)–(15.3.4) satisfied by *all* members of the power classes. Some power class QTFRs of particular importance include the *power Wigner distribution*, the *powergram*, the *smoothed pseudo power Wigner distribution* [7], and the *Bertrand P_κ-distributions* (see Article 7.1 and [2] [7]). All these QTFRs have counterparts in the affine class by virtue of the power warping relation in (15.3.7). For example, the power Wigner distribution,

$$\begin{aligned} W_X^{(\kappa)}(t,f) &= \left|\frac{f}{\kappa}\right| \int_{-\infty}^{\infty} X\left(f\Lambda_\kappa^{-1}\left(1+\frac{\beta}{2}\right)\right) X^*\left(f\Lambda_\kappa^{-1}\left(1-\frac{\beta}{2}\right)\right) e^{j2\pi \frac{tf}{\kappa}\beta} \frac{d\beta}{|1-\frac{\beta^2}{4}|^{\frac{\kappa-1}{2\kappa}}} \\ &= W_{\mathcal{U}_\kappa X}\left(t/(f_r \tau_\kappa(f)),\, f_r\, \Lambda_\kappa(f/f_r)\right), \end{aligned}$$

[2] Unitarity of the operator $\mathcal{U}_\kappa$ implies that $\mathcal{U}_\kappa$ preserves inner products. Specifically, the operator satisfies $\int_{-\infty}^{\infty} (\mathcal{U}_\kappa X)(f)\, (\mathcal{U}_\kappa X)^*(f)\, df = \int_{-\infty}^{\infty} X(f)\, X^*(f)\, df$.

(cf. (15.3.7)) is the power warped version of the well-known Wigner distribution (WD) , $W_X(t,f) = \int_{-\infty}^{\infty} X(f+\frac{\nu}{2})X^*(f-\frac{\nu}{2})\, e^{j2\pi t\nu}\, d\nu$ [3] [4] [5]. As such, it satisfies many properties such as a specific set of marginal properties and the perfect TF localization property for power impulses in (15.3.2). Just like the WD, the power WD contains oscillatory and partly negative cross terms when multicomponent signals are analyzed (see Article 4.2 and [10]). In order to suppress cross terms, a specific type of smoothing can be applied that is matched to the power TF geometry. The powergram and the smoothed pseudo power WD apply such a smoothing to the power WD, at the expense of the loss of some properties (such as the marginal properties) and the loss of TF resolution. The Bertrand P_κ-distributions (see Article 7.1 and [2]) are also perfectly localized for power impulses; moreover, they are the only power class QTFRs that preserve constant time shifts in addition to power dispersive time shifts. Power class members and their properties are discussed in detail in [7]. Next, we present examples with both synthetic and real data.

15.3.2 Power Class Applications

Synthetic data analysis example. The discrete implementation of power QTFRs (outlined in [10] [7]) was applied to analyze a two-component signal consisting of two power impulses with power parameter $\kappa_{\text{signal}} = 3$. For computational purposes, the impulses are windowed in the frequency domain. Figs. 15.2(a) and 15.2(b) show the results obtained with the power WD and a smoothed pseudo power WD with a very short smoothing window. Both QTFRs have power parameter $\kappa = 3$, matched to the power impulse parameter κ_{signal}. The power WD in Fig. 15.2(a) has very good TF concentration but large cross terms [10] which are effectively suppressed in the smoothed pseudo power WD in Fig. 15.2(b) with hardly any loss of TF concentration. Also shown (in Figs. 15.2(c) and 15.2(d)) are the results obtained with the WD and an affine-smoothed pseudo WD, both members of the affine class [4] (i.e., both QTFRs have power parameter $\kappa = 1 \neq \kappa_{\text{signal}}$). The WD in Fig. 15.2(c) is not matched to the power impulses, displaying complicated cross terms. The affine-smoothed pseudo WD in Fig. 15.2(d) does not suppress all the cross terms and has a larger loss of TF concentration than does the smoothed pseudo power WD in Fig. 15.2(b). Although all QTFRs in Fig. 15.2 are scale covariant, the results of the two power QTFRs with $\kappa = 3$ in Figs. 15.2(a) and 15.2(b) are better than those of the two affine QTFRs with $\kappa = 1$ in Figs. 15.2(c) and 15.2(d) because the former two are optimally matched to the $\kappa_{\text{signal}} = 3$ power law group delays of the power impulse signal components.

In order to further demonstrate the effect of mismatch in the signal parameter κ_{signal} and the QTFR power parameter κ, Figs. 15.2(e) and 15.2(f) show the results obtained when analyzing the above signal using the power WD and a smoothed pseudo power WD with QTFR power parameter $\kappa = 4$. Note that in Figs. 15.2(e) and 15.2(f) the power parameter of the power class QTFRs, $\kappa = 4$, is different from that of the signal, $\kappa_{\text{signal}} = 3$. The smoothed pseudo power WD in Fig. 15.2(f) has better cross term suppression and better TF concentration along the true group de-

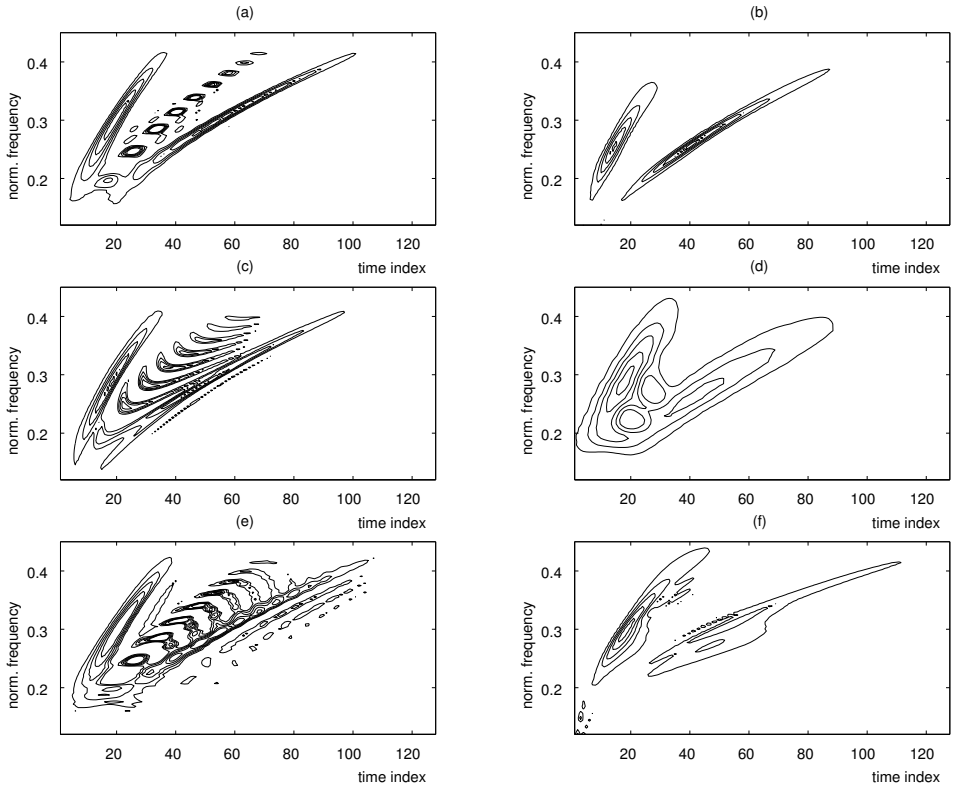

Figure 15.2: Power class analysis of a two-component analytic signal consisting of the sum of two windowed power impulses with signal power parameter $\kappa_{\text{signal}} = 3$. (a) Power WD with $\kappa = 3$, (b) smoothed pseudo power WD with $\kappa = 3$, (c) WD ($\kappa = 1$), (d) affine-smoothed pseudo WD ($\kappa = 1$), (e) power WD with $\kappa = 4$, and (f) smoothed pseudo power WD with $\kappa = 4$.

lay than the affine-smoothed pseudo WD in Fig. 15.2(d) since the power parameter mismatch in Fig. 15.2(f) is smaller than in Fig. 15.2(d).

Real data analysis example. Next, we demonstrate the use of power class QTFRs for analyzing real data with dispersive TF structure. Fig. 15.3 shows two power class QTFRs with $\kappa = 0.35$ and two affine ($\kappa = 1$) QTFRs of the measured impulse response of a steel beam with rectangular cross section[3] [8]. The impulse response was obtained by lightly tapping one end of the steel beam in the direction orthogonal to the flat side of the beam. Bending waves travel along the beam until they are reflected at the free end. They return to the point of impact, are reflected again, etc., thereby producing a series of echoes with increasing dispersion. The QTFRs in Fig. 15.3 display a bandpass-filtered segment of the measured impulse response.

[3]The data was obtained by J. Woodhouse in an experiment at Cambridge University. We are grateful to D. Newland and J. Woodhouse for making this data accessible to us.

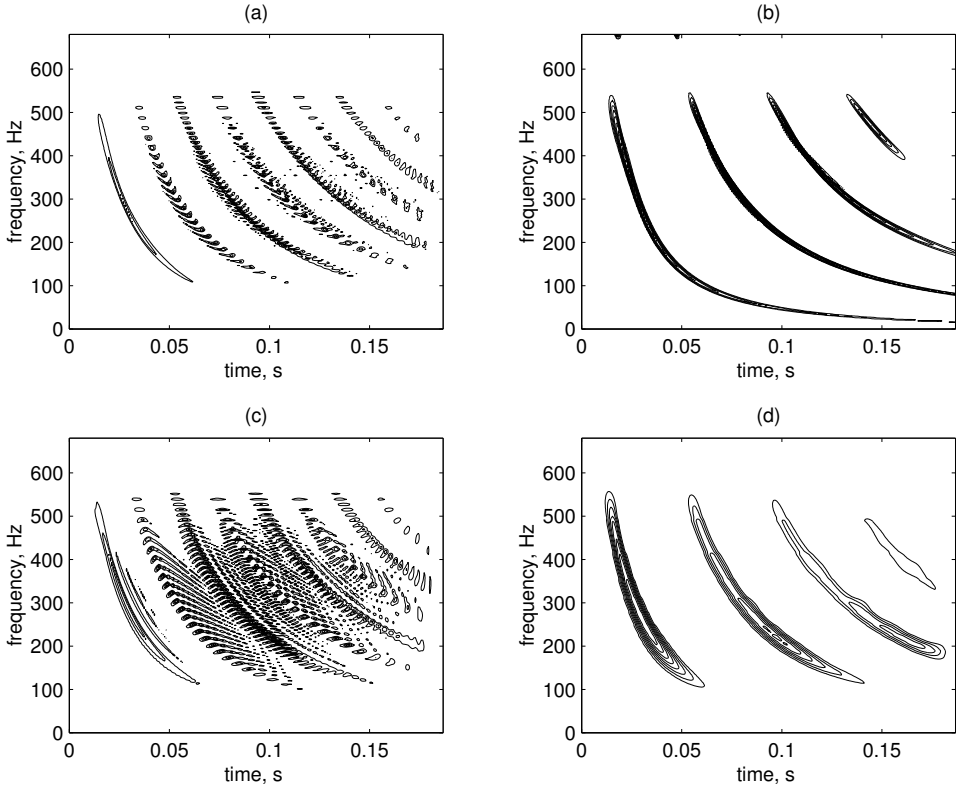

Figure 15.3: Power class analysis of a bandpass-filtered segment of the measured impulse response of a steel beam (sampling frequency 4,096 Hz). (a) Power WD with $\kappa = 0.35$, (b) smoothed pseudo power WD with $\kappa = 0.35$, (c) WD ($\kappa = 1$), and (d) affine-smoothed pseudo WD ($\kappa = 1$).

As can be seen, the smoothed pseudo power WD with $\kappa = 0.35$ in Fig. 15.3(b) shows better resolution and/or cross term suppression than the other three QTFRs depicted. The specific value of $\kappa = 0.35$ was chosen empirically to match the TF curvature of the primary reflection.

15.3.3 Summary and Conclusions

This article presented QTFR classes specifically matched to signals and systems with power law group delay characteristics. These *power* QTFRs preserve scale changes and power law frequency-dependent time shifts of the signal under analysis. Thus, these QTFRs are potentially useful in applications where a propagation medium causes power dispersive time shifts as was demonstrated using a real data example. The implementation of power QTFRs can be based on a warping transformation that relates the κth power class with the affine class. Successful application of power class QTFRs presupposes sufficient *a priori* knowledge about the signal to aid in choosing the appropriate power parameter κ.

References

[1] R. G. Baraniuk and D. L. Jones, "Unitary equivalence: A new twist on signal processing," *IEEE Trans. on Signal Processing*, vol. 43, pp. 2269–2282, Oct. 1995.

[2] J. Bertrand and P. Bertrand, "A class of affine Wigner functions with extended covariance properties," *Journal of Math. Physics*, vol. 33, pp. 2515–2527, 1992.

[3] L. Cohen, *Time-Frequency Analysis.* Englewood Cliffs, NJ: Prentice-Hall, 1995.

[4] P. Flandrin, *Time-Frequency/Time-Scale Analysis.* San Diego, CA: Academic Press, 1999. (Original French edition: *Temps-fréquence.* Hermès, Paris, 1993).

[5] F. Hlawatsch and G. F. Boudreaux-Bartels, "Linear and quadratic time-frequency signal representations," *IEEE Signal Proc. Magazine*, vol. 9, pp. 21–67, April 1992.

[6] F. Hlawatsch, A. Papandreou-Suppappola, G. F. Boudreaux-Bartels, "The hyperbolic class of quadratic time-frequency representations Part II: Subclasses, intersection with the affine and power classes, regularity, and unitarity," *IEEE Transactions on Signal Processing*, vol. 45, pp. 303–315, February 1997.

[7] F. Hlawatsch, A. Papandreou-Suppappola, and G. F. Boudreaux-Bartels, "The power classes—quadratic time-frequency representations with scale covariance and dispersive time-shift covariance," *IEEE Transactions on Signal Processing*, vol. 47, pp. 3067–3083, November 1999.

[8] D. E. Newland, "Time-frequency and time-scale analysis by harmonic wavelets," Chapter 1 of *Signal Analysis and Prediction*, A. Prochazka et al. (eds.). Boston, MA: Birkhäuser, 1998.

[9] A. Papandreou, F. Hlawatsch, and G. F. Boudreaux-Bartels, "The hyperbolic class of quadratic time-frequency representations, Part I: Constant-Q warping, the hyperbolic paradigm, properties, and members," *IEEE Transactions on Signal Processing*, vol. 41, pp. 3425–3444, December 1993.

[10] A. Papandreou-Suppappola, F. Hlawatsch, and G. F. Boudreaux-Bartels, "Power class time-frequency representations: Interference geometry, smoothing, and implementation," Proceedings of the *IEEE-SP International Symposium on Time-Frequency and Time-Scale Analysis*, (Paris, France), pp. 193–196, June 1996.

[11] A. Papandreou-Suppappola, F. Hlawatsch, G. F. Boudreaux-Bartels, "Quadratic time-frequency representations with scale covariance and generalized time-shift covariance: A unified framework for the affine, hyperbolic and power classes," *Digital Signal Processing: A Review Journal*, vol. 8, pp. 3–48, January 1998.

[12] O. Rioul and P. Flandrin, "Time-scale energy distributions: A general class extending wavelet transforms," *IEEE Transactions on Signal Processing*, vol. 40, pp. 1746–1757, July, 1992.